

Journal of Advanced Research Design



Journal homepage: https://akademiabaru.com/submit/index.php/ard ISSN: 2289-7984

An Enhanced Very-Deep Super-Resolution (VDSR) Neural Network for Single Image Super-Resolution using Luminance and Chrominance Channels

Mazlinda Ibrahim^{1,*}, Muhammad Anas Zulkeffly², Mat Kamil Awang², Hoo Yann Seong¹, Nurul Kamilah Mat Kamil³

- ¹ Centre for Defence Foundation Studies, National Defence University of Malaysia, 57000 Kuala Lumpur, Malaysia
- Department of Electrical and Electronic Engineering, Faculty of Engineering, National Defence University of Malaysia, 57000 Kuala Lumpur, Malaysia
- ³ Faculty of Electrical Engineering and Information Technology, RWTH Aachen, Aachen, Germany

ARTICLE INFO

ABSTRACT

Article history:

Received 27 March 2025 Received in revised form 18 August 2025 Accepted 29 September 2025 Available online 10 October 2025 Single Image Super-Resolution (SISR) is a fundamental problem in computer vision, aiming to enhance the resolution of a low-resolution image while preserving its details and structure. The Very-Deep Super-Resolution (VDSR) network has demonstrated significant success in SISR tasks due to its depth and residual learning framework. However, its performance can be further improved by utilizing additional image information. In this paper, we propose an enhanced VDSR network that integrates luminance and chrominance channels as supplementary inputs. By separately processing the luminance and chrominance components, the network learns complementary features, enabling more accurate reconstruction of highfrequency details and textures. This approach aligns with the human visual system's heightened sensitivity to brightness changes, resulting in super-resolved images with superior perceptual quality. Experimental results on available datasets confirm that the proposed method outperforms the original VDSR, achieving notable improvements in natural image quality evaluator, blind image spatial quality evaluator and perception-based image quality evaluator. The decrease in the performance metrics is up to 2%. This study underscores the effectiveness of incorporating luminance and chrominance information in SISR tasks, paving the way for more accurate and visually appealing image reconstructions.

Keywords:

Super Resolution; Neural Network; Image Restoration; Image Reconstruction; Perceptual Quality

1. Introduction

Super Resolution (SR) is one of the crucial tasks in image processing. The task is closely related to image upscaling, image enhancement, and image reconstruction. In SR, high resolution (HR) images are obtained from the low-resolution (LR) images. Single Image Super-Resolution (SISR) is the process of generating HR images from LR images using only the information available within the image itself

E-mail address: mazlinda@upnm.edu.my

https://doi.org/10.37934/ard.145.1.122135

 $[^]st$ Corresponding author.

while preserving the fine details and textures. SISR has many applications and potential usage such as in crack detection in marine concrete structure monitoring system [1] and in application of remote sensing images [2]. According to Azam *et al.* [3], despite the numerous SISR methods proposed over the years, further development is still necessary. The improvements can be made to enhance the quality of the HR image generated from an LR image, particularly in areas such as edge structure, artifact reduction, and textural quality.

Traditional SISR methods can be broadly categorized into interpolation, reconstruction, and example based methods. Interpolation-based methods, such as bilinear and bicubic interpolation, are simple and computationally efficient but often produce blurry results due to their inability to recover high-frequency details. Reconstruction-based methods used prior knowledge about the image formation process to reconstruct HR images. However, these methods are computationally expensive and sensitive to noise. Example-based methods, pioneered by Freeman *et al.* [4], used a database of LR-HR image pairs to learn the mapping between them. These methods can produce sharper results but are limited by the quality and diversity of the training dataset.

According to Mustafa *et al.* [5] image quality assessment (IQA) is typically divided into two categories: subjective and objective measurements. Objective IQA involves automatically predicting the perceived quality of distorted images as judged by the average human observer. While subjective evaluation, such as the mean opinion score (MOS), provides the most definitive results, it is often impractical due to its time-consuming and costly nature. As a result, objective metrics like mean squared error (MSE) and peak signal to noise ratio (PSNR) have been developed as faster alternatives. However, these objective methods do not always correlate well with MOS. In addition, according to Qiu *et al.* [6], both MSE and PSNR fail to consider human visual effects. Furthermore, according to Jiang *et al.* [7], the most popular IQA is PSNR, however, it suffers from low correlation with human perception.

Meanwhile, perceptual image quality assessment (PQA) is closely related to the subjective measurements. PQA aims to mimic human perception using computational models. PQA focuses on factors like sharpness, contrast, texture, and naturalness to align with human subjective experience. PQA can be classified into: Full-Reference (FR), Reduced-Reference (RR) and No-Reference (NR). FR compares the distorted image with a high-quality reference image. RR uses partial information from the reference image for assessment. NR evaluates image quality without a reference image. For example, Natural Image Quality Evaluator (NIQE) [8], Blind/Referenceless Image Spatial Quality Evaluator (BRISQUE) [9], and Perception-based Image Quality Evaluator (PIQE) [10].

NR IQA metrics are designed to assess image quality without relying on a reference image. Compared to FR and RR IQA, NR IQA is more challenging due to the lack of prior information. However, this also makes NR IQA methods highly appealing for practical applications as mentioned by Zai and Xiongkuo in [11]. In addition, BRISQUE has minimal computational complexity, making it highly suitable for real-time applications as highlighted by Mustafa *et al.* in [5]. In 2022, Catalbas [12] emphasizes the importance of NR-IQA methods, particularly NIQE, in evaluating image quality without the need for a reference image. The author demonstrated that NIQE is effective in detecting image distortion and optimizing the SISR process.

PQA is inspired by subjective IQA but is often implemented as an objective metric that approximates human perception. Based on the literature, the majority of the IQA used in SISR are PSNR and structural similarity index (SSIM) [1,3,12,13,14,15]. One might argue that SSIM is PQA, however, according to Pambrun and Rita [16], SSIM has been increasingly criticized for its limitations in accurately reflecting human visual perception, especially in medical imaging contexts. Additionally, Wang *et al.* [17] highlighted that SSIM, while considering structural information, may not fully account for all aspects of human visual perception, leading to discrepancies between SSIM scores

and perceived image quality. Therefore, although SSIM incorporates some perceptual considerations, it does not entirely align with human perception, and more advanced metrics are required for comprehensive perceptual quality assessment.

Channels in digital images refer to the separate component of the image which represents a specific aspect of colour or intensity. Two most common channels in digital images are RGB and YCbCr. RGB refers to red, green, and blue colour model. Meanwhile, YCbCr consists of luminance (Y), and two chrominance (CbCr) channels. The human visual system is more sensitive to changes in luminance than to changes in chrominance. This observation has led to the development of image processing techniques that separately process luminance and chrominance channels. For example, in video compression standards luminance is given higher priority than chrominance to achieve better perceptual quality.

In 2014, Dong et al. [18] proposed SISR based on convolutional neural network (CNN) called super resolution convolutional network (SRCNN) [18]. However, the IQA used in [18] are PSNR, SSIM, noise quality measure, weighted peak signal-to-noise ratio and multi-scale structure similarity index. Another interesting highlight from [18] is they demonstrated that performance of SRCNN can be improved in comparison to the single channel network, since most of the SR methods focus on grayscale or single channels SR. Furthermore, Zhang et al. [19] proposed a method that separately processes luminance and chrominance channels to improve the perceptual quality of super-resolved images. Their results demonstrated that incorporating luminance and chrominance information can lead to more visually appealing reconstructions.

The Very Deep Super-Resolution (VDSR) developed by Kim *et al.* [20] is a widely recognized approach in SISR. In the literature, VDSR is among the most popular CNN based SR techniques, and this study focuses on enhancing its performance. VDSR employs a deep network architecture with residual learning, which allows it to capture high-frequency details effectively. Despite the success of deep learning-based SISR methods, there remains a significant research gap in leveraging luminance and chrominance information to improve the perceptual quality of super-resolved images. While VDSR and other deep learning models have achieved impressive results in terms of PSNR and SSIM, they primarily focus on processing RGB images, potentially overlooking the importance of luminance and chrominance channels.

Iriyama et al. [21] explored the strategy of processing luminance and chrominance channels separately in the context of image demosaicking. In their 2021 work, they introduced a novel CNN-based method that independently estimates these components. Their approach demonstrated competitive performance compared to state-of-the-art demosaicking techniques, while also reducing computational complexity. Similarly, Claßen and Wien [22] proposed an image filtering scheme for image upscaling that utilizes an adaptive weighted filter based on luminance and chrominance channels. Their method achieved notable performance improvements over existing techniques.

In this paper, we propose an enhanced VDSR network that incorporates luminance and chrominance channels as additional inputs. By leveraging the human visual system's sensitivity to brightness and colour changes, our approach aims to improve the perceptual quality of superresolved images. Overall, the contributions of this study are mainly in two aspects. First, we present an enhanced VDSR for SISR by utilizing the additional two chrominance channels in YCbCr colour channel. Second, we compare the performance of the enhanced VDSR with the traditional bicubic interpolation method and the original VDSR [20] using the NR PQA which are NIQE [8], BRISQUE [9] and PIQE [10]. Experimental results demonstrate that the proposed method outperforms the original VDSR in terms of NIQE, BRISQUE and PIQE metrics by at most 2% in terms of the percentage of reduction of the performance metrics.

The structure of this paper is as follows: in the second section, we reviewed the bicubic interpolation, the VDSR in [20] and the proposed enhanced VDSR. In the third section, the performance comparison for all three methods is made using three performance metrics. Conclusions of this paper are described in the last section.

2. Methodology

Let the LR image be denoted as X = X(i,j) where (i,j) are integer pixel coordinates. Let Y be the HR image where we wish to recover Y which is as like the ground truth HR image. For non-integer (i,j), we compute Y(p,q) using bicubic interpolation as follows:

$$Y^{Bicubic}(p,q) = \sum_{i=-1}^{2} \sum_{j=-1}^{2} X(m+i,n+j) \cdot W(p-(m+i)) \cdot W(q-(n+j))$$
 (1)

where (m, n) is the nearest integer grid point to (p, q) and W(t) is the bicubic interpolation kernel as follows:

$$W(t) = \begin{cases} (a+2)|t|^3 - (a+3)|t|^2 + 1, & 0 \le |t| < 1\\ a|t|^3 - 5a|t|^2 + 8at - 4a, & 1 \le |t| < 2\\ 0, & |t| \ge 2 \end{cases}$$
 (2)

where a=-0.5 in Eq. (2). Bicubic interpolation for 2D images are performed in two steps. First, the interpolation in the x axis (horizontal direction). Second the interpolated value from the first step is interpolated again in the y-axis (vertical direction). VDSR learns a mapping function from LR to HR images using a deep CNN inspired by VGG-net. It estimates the residual image, R(p,q) where

$$Y^{VDSR}(p,q) = Y^{Bicubic}(p,q) + R(p,q)$$
(3)

and $Y^{Bicubic}(p,q)$ is given in Eq. (1).

Figure 1 illustrates the VDSR network structure. The network consists of 20 weight layers and is trained using 41×41 image patches for HR image reconstruction. It is designed to handle multiple scale factors effectively. The LR image is first upsampled using bicubic interpolation, producing an initial HR estimate: $Y^{Bicubic}(p,q)$. This estimate is then passed through 20 convolutional layers, each followed by a Rectified Linear Unit (ReLU) activation function, enabling the network to learn the residuals between the upsampled image and the HR image. By focusing on residual learning, VDSR improves training efficiency and reconstruction accuracy. The final HR image: $Y^{VDSR}(p,q)$ is obtained by adding the learned residuals: R(p,q) back to the initial estimate: $Y^{Bicubic}(p,q)$.



Fig. 1. VDSR network structure

For example, the LR image in Figure 2 (top left) is 45x66 pixels serves as an input. The initial estimate shown in Figure 2 (top right) using bicubic interpolation with resolution 135x198 where the scale factor is 3. The image passes through 20 convolutional layers, where features such as edges and

textures are extracted and refined. Each layer applies filters to detect patterns, followed by a ReLU activation function to introduce non-linearity and improve learning. Then, the network predicts the residual details for the luminance channel. For instance, the residual image is shown in Figure 2 (bottom left). Then, the residual is added to the HR bicubic to produce the final HR VDSR as shown in Figure 2 (bottom right).

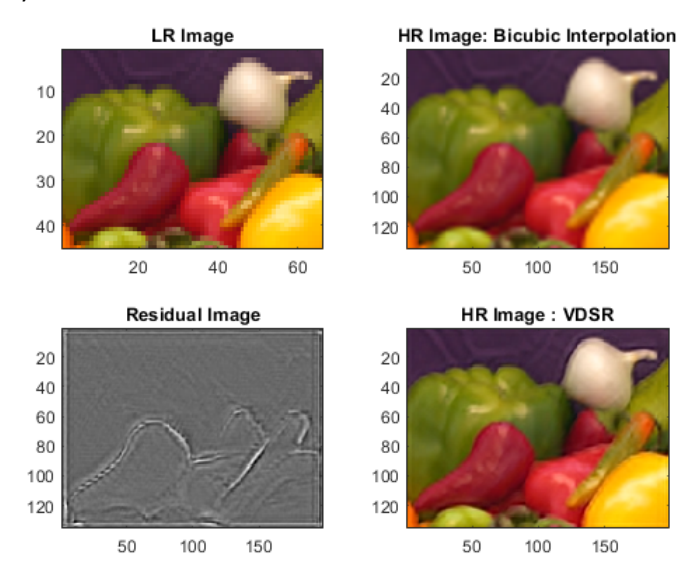


Fig. 2. Examples for the LR, HR using bicubic interpolation, VDSR and residual image

Figure 3 shows the enhanced VDSR pipeline, which incorporates an additional processing step using the two chrominance channels (Cb and Cr) compared to the standard VDSR approach. First, the RGB LR image serves as an input. Second, the image is converted to the YCbCr color space, where the luminance (Y) and chrominance (Cb, Cr) channels are separated. Third, bicubic interpolation is applied to upsample the entire YCbCr channels to the desired HR size. This is followed by the channel separation where the luminance (Y) and chrominance channels are extracted and fed into the VDSR network. The original VDSR in [20] preserved the chrominance (Cb, Cr) channels separately. The fourth step producing three residual images corresponds to Y, Cb and Cr channels. The original VDSR only produces one residual image for the Y channel. Fifth, the VDSR network enhances the three channels, learning fine details and improving image quality. Then, the reconstruction to the RGB image to obtain the final HR image. In the original VDSR, the enhanced Y channel is combined with the bicubic upsampled Cb and Cr channels, then converted back to the RGB color space, producing the final high-resolution output. This enhanced VDSR approach leverages the luminance and chrominance channels.

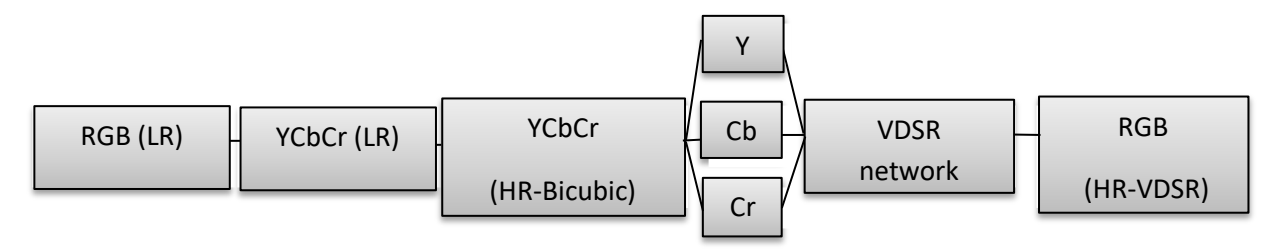


Fig. 3. Enhanced VDSR pipeline

3. Results

In this section, we used 20 images from The Image Processing Toolbox in MATLAB. The images are shown in Figure 4.

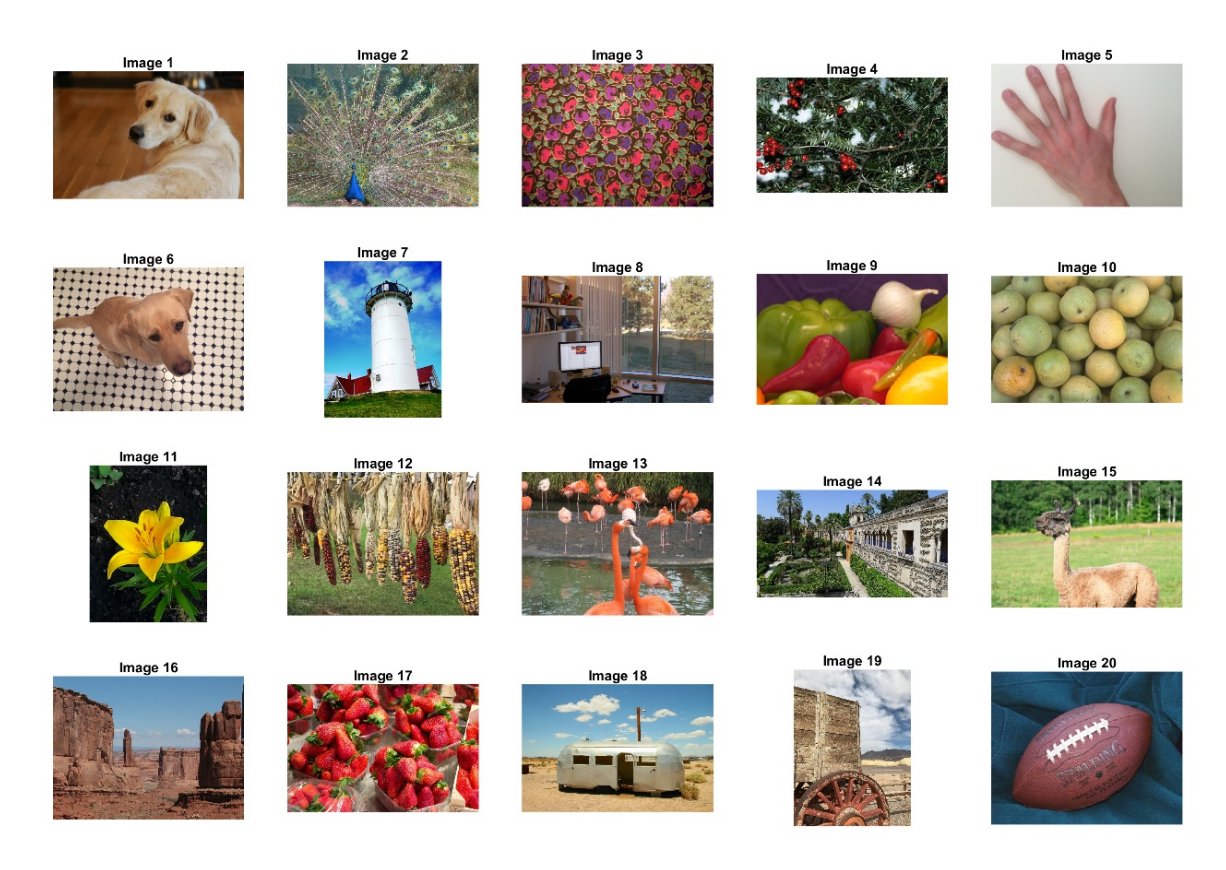


Fig. 4. 20 test images used in the experiment where the images are available from MATLAB

In Figure 4, the HR images are obtained from the LR images for scale factor 2,3, and 4. The scale factor is calculated as follows:

$$Scale = \frac{HR}{LR} \tag{4}$$

where HR and LR in Eq. (4) refer to the resolution of HR and LR image respectively. The experiment is conducted by using MATLAB R2023a software with MATLAB Image Processing Toolbox on Windows 10. The CPU processor used was Intel® Core ™ i7-6700 CPU @ 3.40GHz with 16G RAM. We followed the NR-IQA in [23] which are NIQE, BRISQUE and PIQE. The NIQE compares an image, I to a predefined model derived from natural scene images from database used for training in Mittal *et al.* [8] by leveraging the multidimensional Gaussian distributions functions. A lower value for NIQE indicating better perceptual quality. Similarly, smaller BRISQUE [9] and PIQE [10] values indicates better perceptual quality.

The NIQE values for three methods are shown in Figure 5 for scale factor 2 for image 1 until 20 in Figure 4. From the figure, one may observe that the NIQE values for VDSR and enhanced VDSR (E-VDSR) are comparable. Nearly half of the images exhibit a lower NIQE value with bicubic interpolation than VDSR and enhanced VDSR. For scale factor 2, bicubic interpolation outperforms the other two methods.

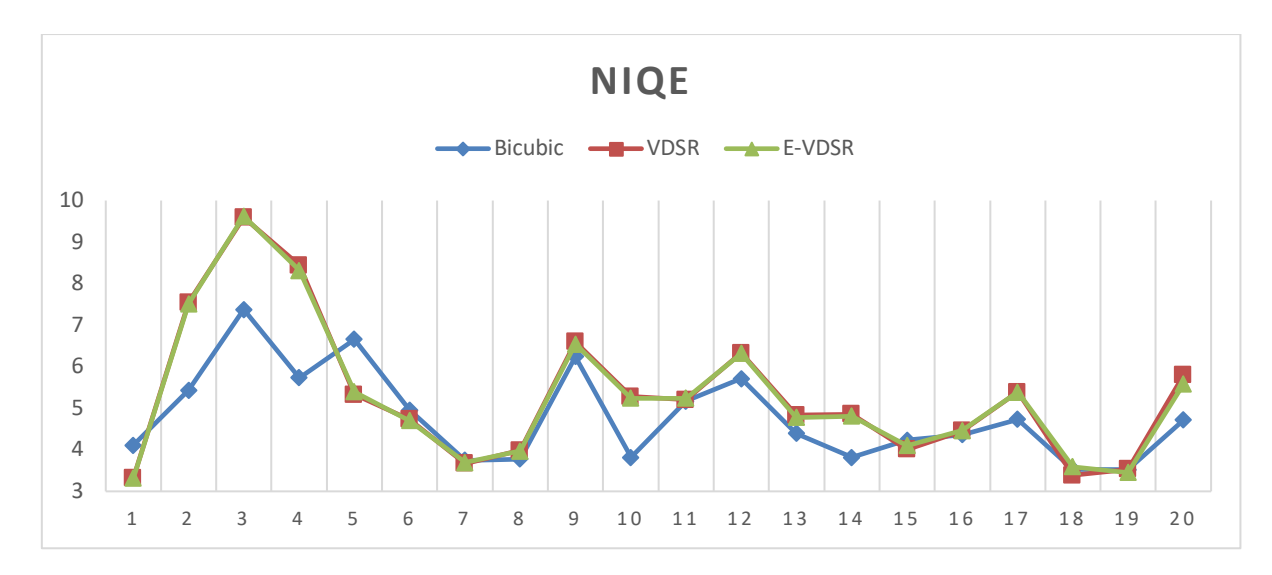


Fig. 5. The NIQE values for three methods: bicubic, VDSR and enhanced VDSR for scale factor 2

Figure 6 shows the NIQE values for scale factor 3. Form the figure, the enhanced VDSR consistently achieves lower NIQE scores compared to both bicubic and original VDSR, indicating better perceptual quality for image 9 and 14. While bicubic interpolation tends to yield higher NIQE values, the deep learning-based methods demonstrate improved visual quality across most images.

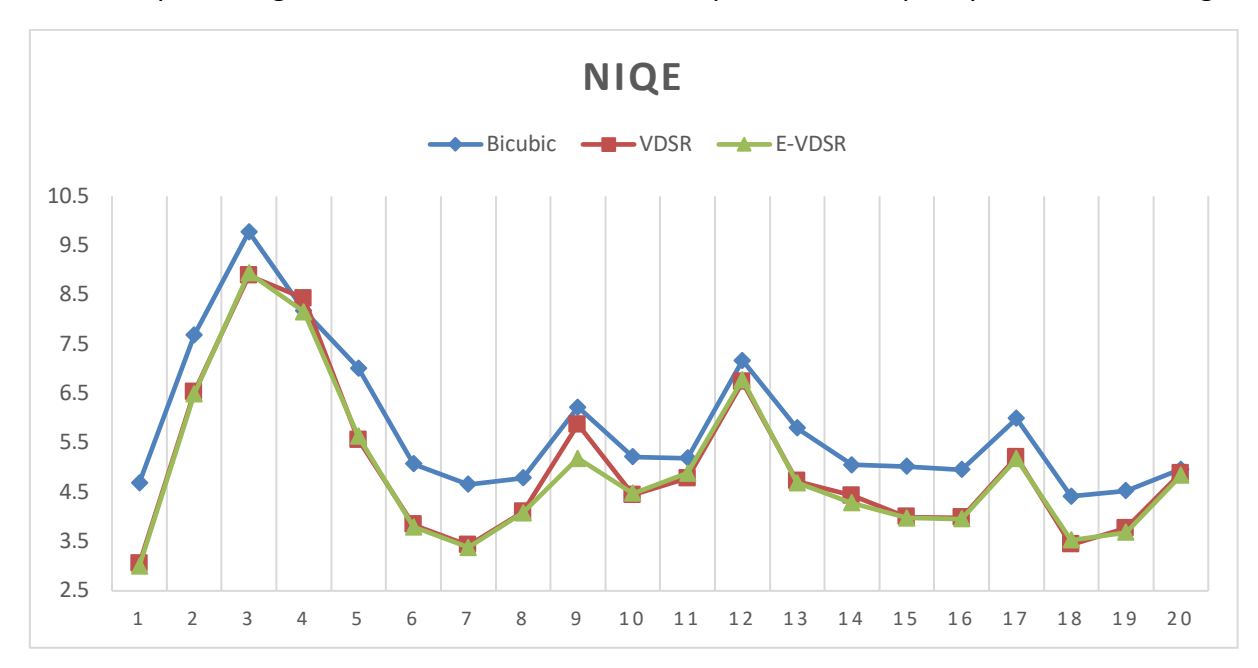


Fig. 6. The values of the NIQE for three methods: bicubic, VDSR and enhanced VDSR for scale factor 3

As shown in Figure 7, the NIQE values for all three methods vary across the 20 test images for scale factor 4. The bicubic interpolation method exhibits the highest NIQE values for all images. The enhanced VDSR consistently achieves the lowest NIQE scores, indicating superior perceptual quality compared to the other two methods for image 9. This suggests that the enhancements introduced in the enhanced VDSR contribute significantly to preserving natural image statistics and reducing perceptual distortion at scale factor of 4.

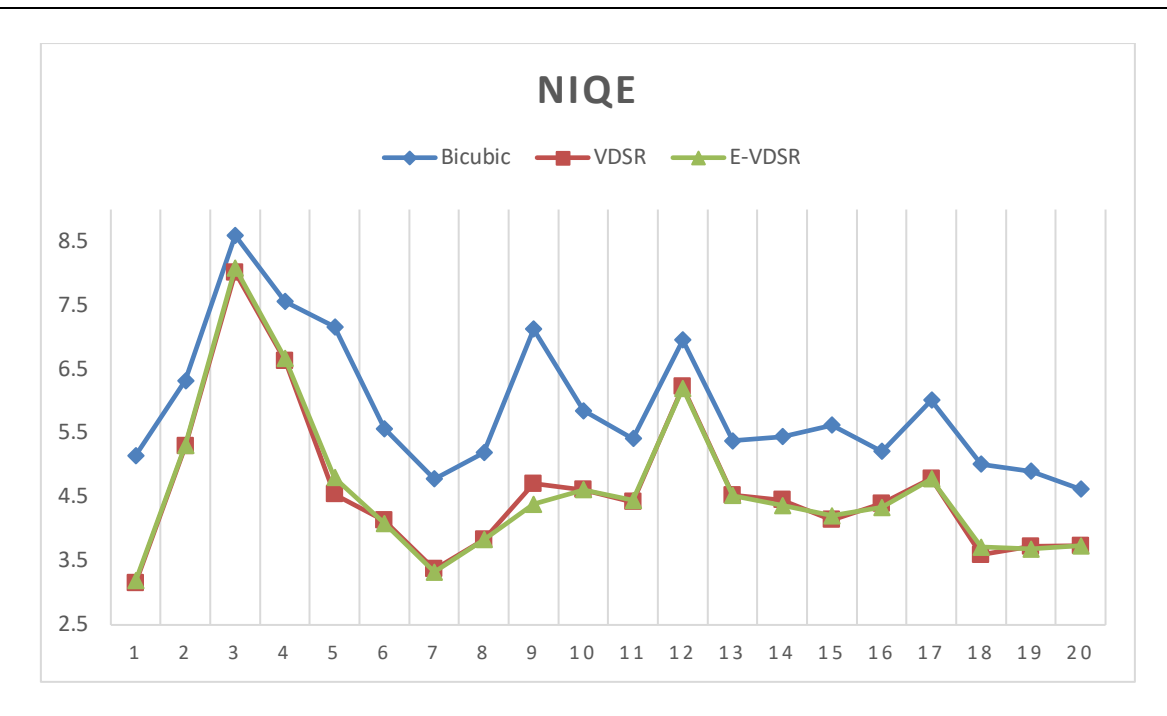


Fig. 7. The values of the NIQE for three methods: bicubic, VDSR and enhanced VDSR for scale factor 4

Figure 8 shows the BRISQUE scores for 20 test images using three methods for scale factor 2. The score between 0 and 30 indicates the images are high quality, while score between 30 and 50 indicates moderate quality. In general, the enhanced VDSR yields lower BRISQUE values compared to both the bicubic and VDSR, indicating improved perceptual image quality for image 1 and 13. The bicubic method consistently produces the highest BRISQUE scores for majority of the images, reflecting greater distortion and lower visual quality.

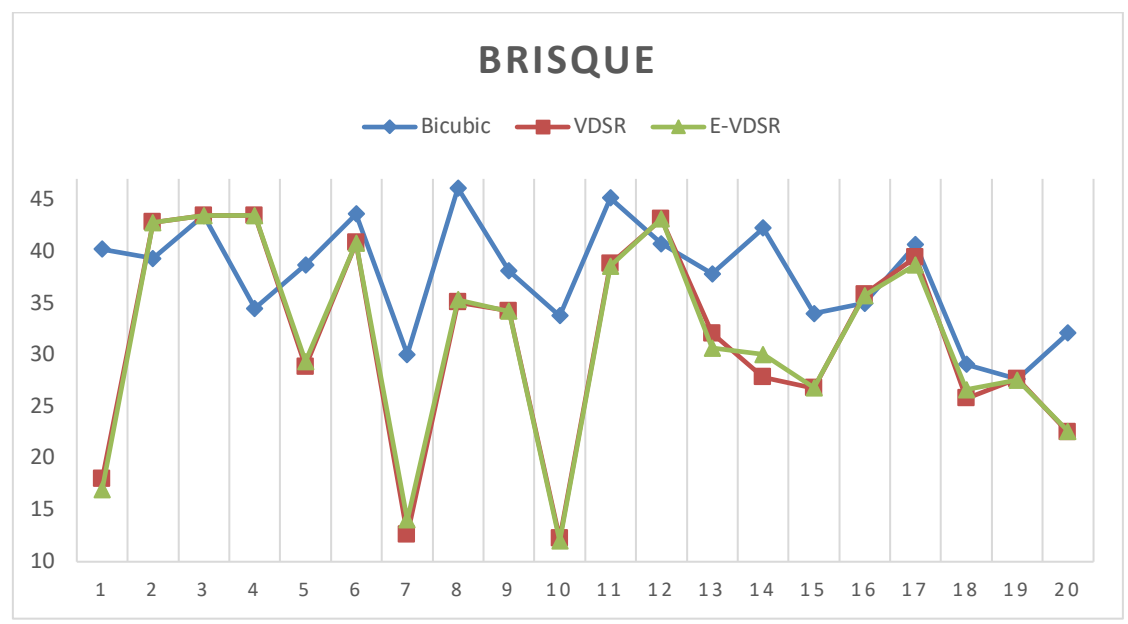


Fig. 8. The values of the BRISQUE for three methods: bicubic, VDSR and enhanced VDSR for scale factor 2

Figures 9 and 10 show the values of the BRISQUE for scale factor 3 and 4 respectively. Based on the figures, one can observe that the enhanced VDSR showed competitive performance with the original VDSR. However, the range of the BRISQUE scale is increasing. For BRISQUES scale above 50, the image is said to have poor perceptual image quality where the visible distortions are presence.

Based on Figure 9, the bicubic interpolation method is at disadvantages compared to the VDSR methods. In addition, the enhanced VDSR shows lower BRISQUE score for image 7,9 ,11, 14,16 and 18 compared to the original VDSR method.

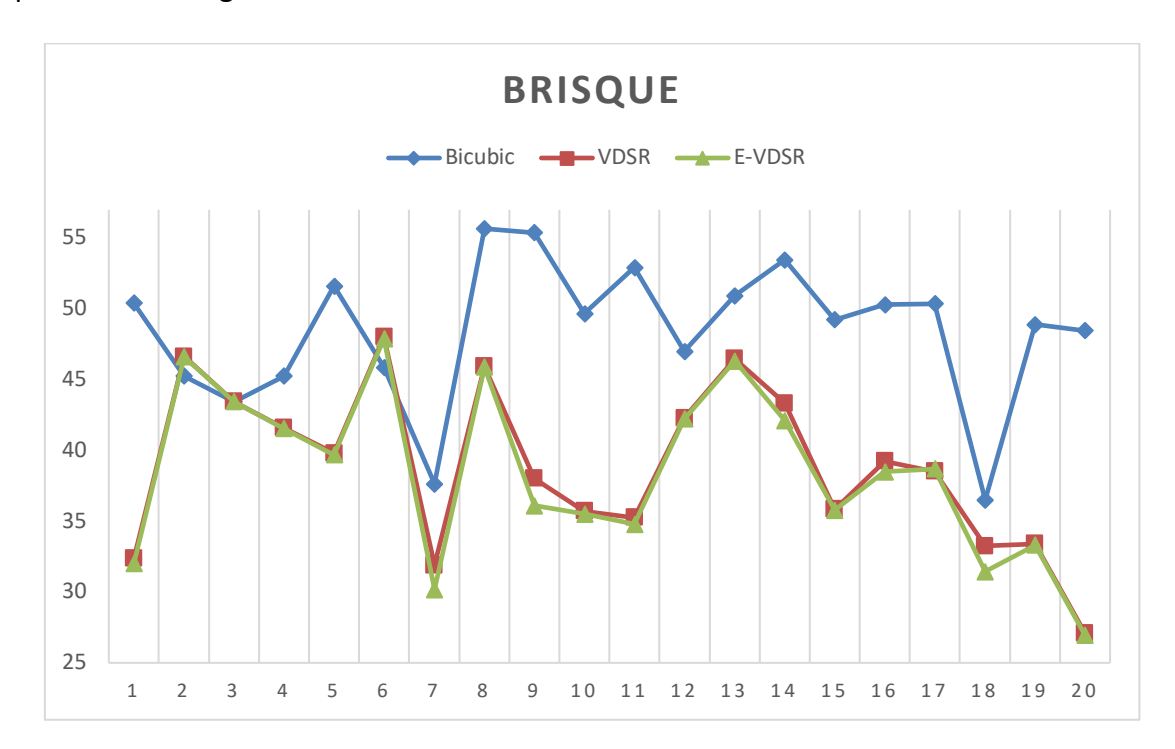


Fig. 9. The values of the BRISQUE for three methods: bicubic, VDSR and enhanced VDSR for scale factor 3

Similarly, in Figure 10, the bicubic interpolation method show higher values of the BRISQUE scores for scale factor 4. Meanwhile, the enhanced VDSR method has lower BRISQUES score compared to the original VDSR method for image 5, 9 and 18. The enhanced VDSR method show significant improvement in such images.

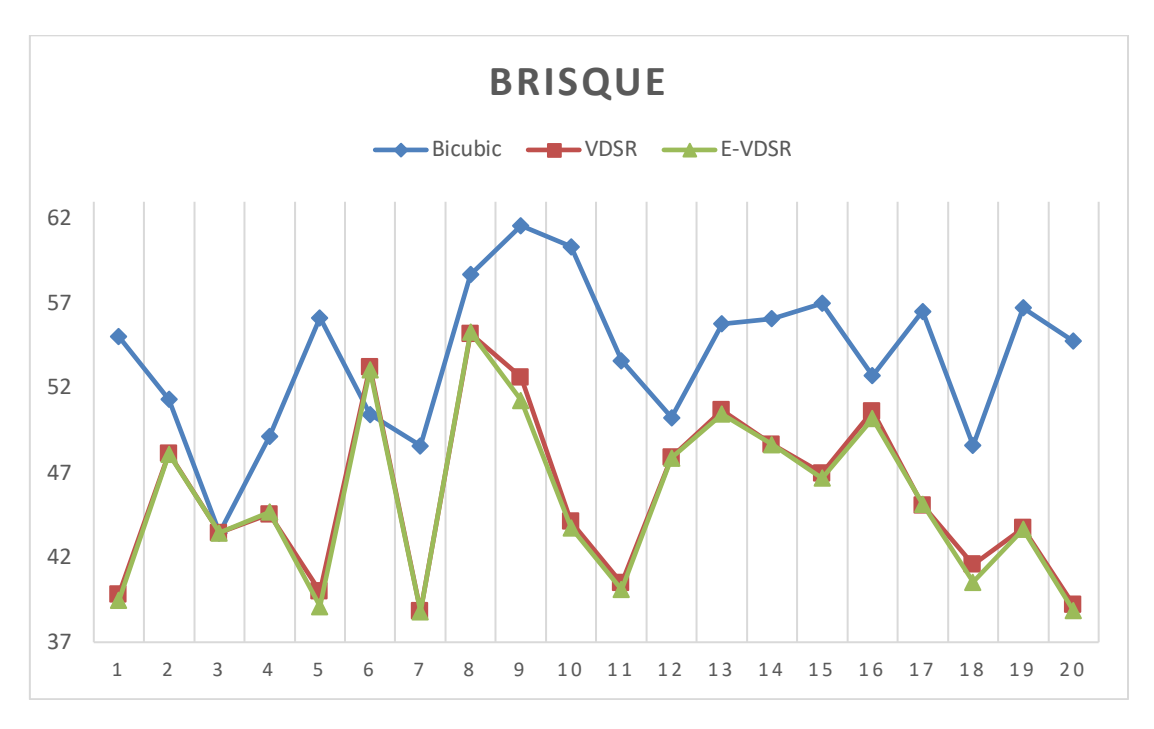


Fig. 10. The values of the BRISQE for three methods: bicubic, VDSR and enhanced VDSR for scale factor 4

Figures 11, 12 and 13 show PIQE values for scale factor 2, 3 and 4 respectively. Notice that the values of the enhanced VDSR have smaller PIQE values than the VDSR for image no. 5, 6 and 7 for scale factor 2. Overall, the enhanced VDSR and original VDSR outperformed the bicubic interpolation method. From Figure 11, the PIQE scores for bicubic interpolation method are higher for all images. The minimum score is 31 and the maximum score is 85. Meanwhile, the range for the VDSR methods are between 8 and 42.

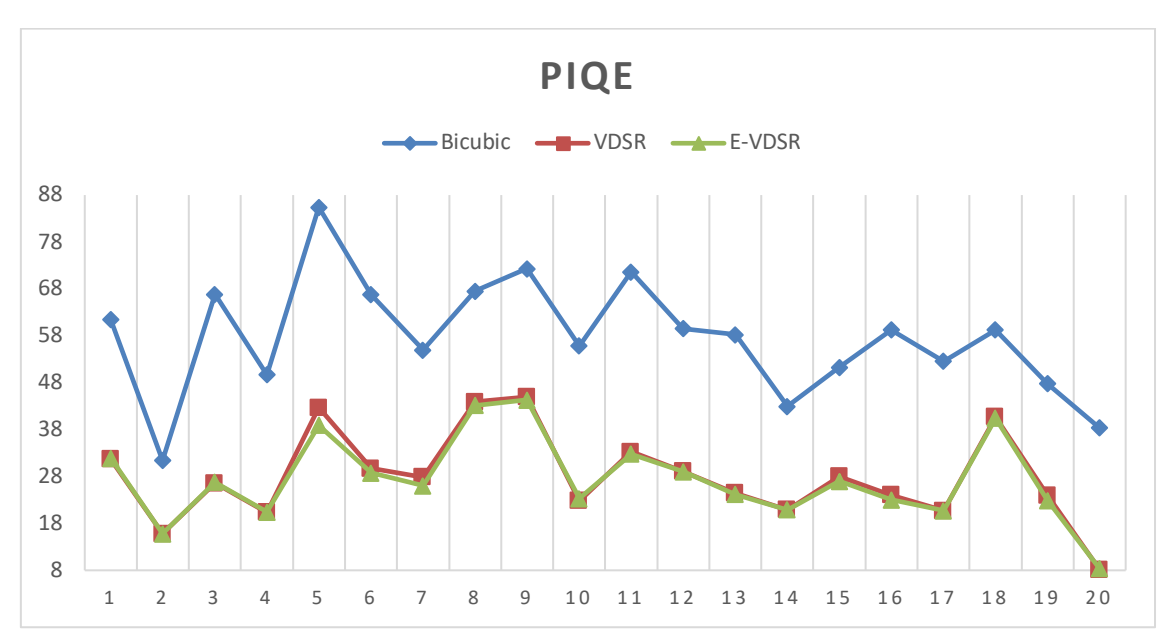


Fig. 11. The values of the PIQE for three methods: bicubic, VDSR and enhanced VDSR for scale factor 2

Figure 12 shows the PIQE score for scale factor 3. Similar observations can be made where the bicubic interpolation shows higher values of the PIQE scores compared to the VDSR methods. In addition, the enhanced VDSR exhibit lower PIQE scores for most of the images. This clearly highlights the improvement over the original VDSR.

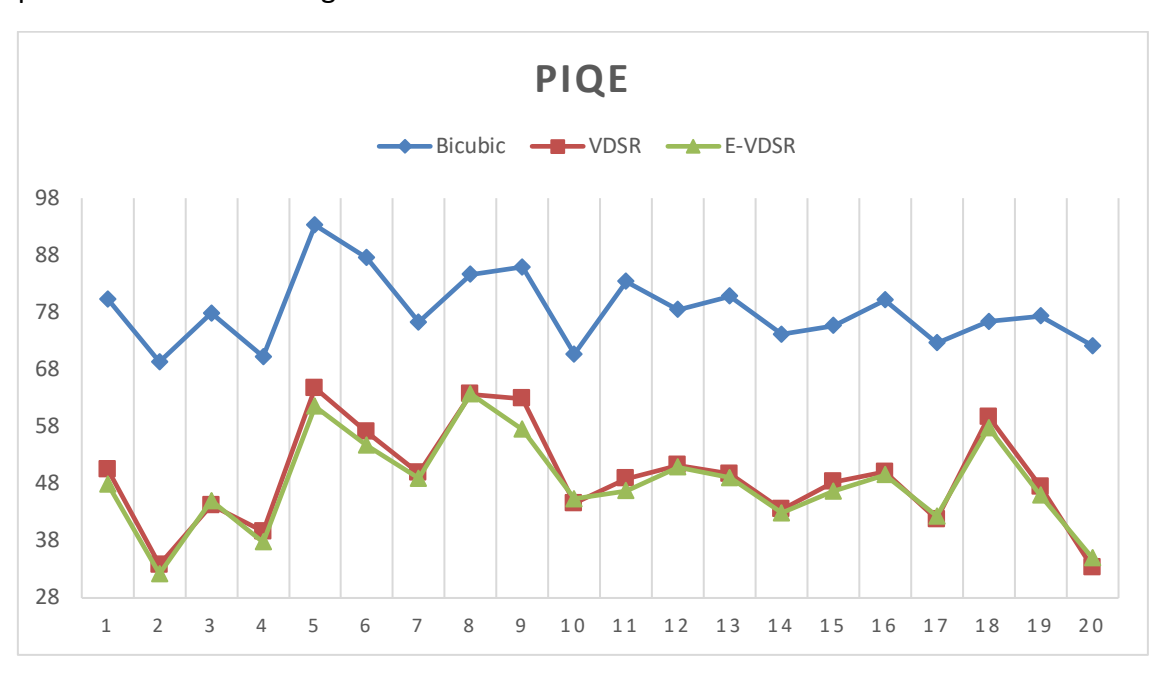


Fig. 12. The values of the PIQE for three methods: bicubic, VDSR and enhanced VDSR for scale factor 3

Figure 13 shows the PIQE scores for scale factor 4. From Figure 13, the enhanced VDSR has a lower value of PIQE than VDSR for most images. Overall, both VDSR and enhanced VDSR surpass the bicubic interpolation method.

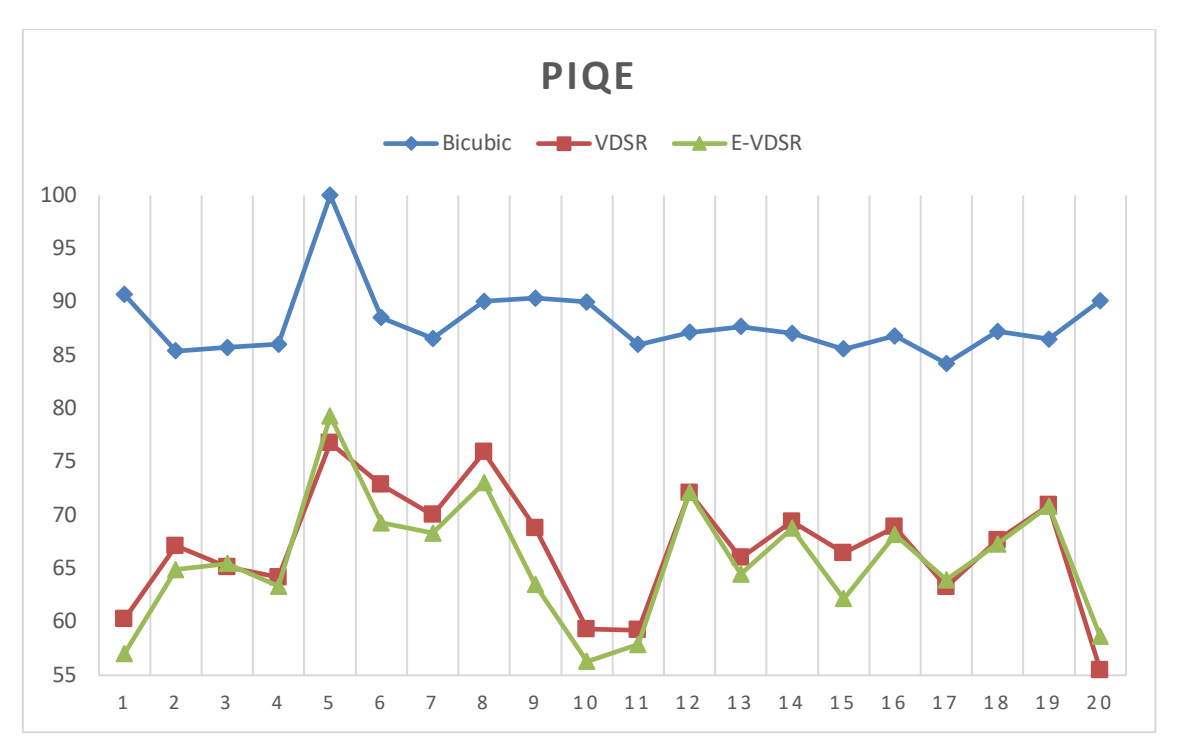


Fig. 13. The values of the PIQE for three methods: bicubic, VDSR and enhanced VDSR for scale factor 4

Bicubic interpolation reconstructs missing pixels by applying a weighted sum of neighbouring pixels using a fixed cubic kernel function, W(t) as shown in Eq. (3). Since bicubic only uses local pixel information, it struggles to reconstruct high-frequency details, leading to blurring and loss of texture as the scale factor increases. At scale factor 2, bicubic may still provide acceptable results, but as the scale factor increases, the limitations of bicubic interpolation become more apparent. Unlike bicubic, VDSR and enhanced VDSR learn to reconstruct textures and edges from a large dataset, significantly improving perceptual quality at large upscaling factors. The deep learning capability in both methods, effectively restores fine details and textures, leading to sharper and more visually appealing high-resolution images.

For more quantitative measurements of the performance metrics, we calculated the average relative percentage of reduction for the original VDSR and the proposed enhanced VDSR. The relative percentage of reduction metrics are calculated as follows:

$$PR\% = \frac{(A-B)}{A} \times 100$$

where A and B are the values for the performance metrics (NIQE, BRISQUE and PIQE) corresponding to VDSR and enhanced VDSR respectively. From Table 1, the relative percentage of reduction of the NIQE at scale 2 is very small at 0.05%, indicating minimal improvement. However, at scale 3, there's a significant reduction of 1.04% which suggesting enhanced VDSR performs better than the original VDSR. Meanwhile, at scale 4, the reduction is lower at only 0.01% which implying limited improvement at high upscaling. The biggest improvement of NIQE scores occurs at scale 3, while at scale 2 and scale 4, the enhancements are minor.

The relative percentage of reduction of the BRISQUE at scale 2 is negative at -0.47%, meaning enhanced VDSR slightly worsened performance compared to the original VDSR. At scale 3, there's a noticeable reduction of 1.27%, indicating an improvement and at scale 4, the reduction is at 0.64% which is moderate improvement. The relative percentage of reduction of the PIQE at scale 2 is 1.56%, which show improvement where the highest reduction is 2.11% which shown at scale 3. At scale 4, the reduction remains high which is 1.86%, confirming improvement compared to the original VDSR.

Table 1Average values for the relative percentage of reduction of the performance metrics for scale 2,3 and 4

Scale	2	3	4
NIQE	0.04538	1.040501	0.014712
BRISQUE	-0.47195	1.268679	0.635834
PIQE	1.558912	2.107133	1.858087

The enhanced VDSR method is most effective at scale 3, showing clear benefits in perceptual quality. At scale 2, the low-resolution image already has sufficient details, making it harder for enhanced VDSR to show noticeable improvements. Instead, over-enhancement, noise, or artifacts may slightly degrade perceptual quality. However, at higher scale factors for example at scale 3 and 4, where more details are missing, enhanced VDSR significantly improves image quality, leading to better performance across all metrics.

4. Conclusions

In this study, we proposed an enhanced VDSR network that incorporates both luminance and chrominance channels to improve the performance of SISR. Unlike the conventional VDSR model that primarily focuses on the luminance channel, our method leverages the complementary nature of luminance and chrominance information to guide the reconstruction process more effectively. By explicitly modeling the inter-channel relationships, the network can recover fine grained textures and intricate image structures, which are often lost in traditional luminance only approaches.

Through extensive experiments across multiple images in the datasets, the proposed model consistently outperformed the original VDSR in both qualitative and quantitative evaluations. In particular, the results show substantial improvements in no-reference image quality assessment metrics, namely NIQE, BRISQUE, and PIQE, indicating that the reconstructed images are not only more accurate but also more perceptually pleasing to human observers. These improvements underscore the importance of integrating full color information in deep learning based SISR models, especially for applications where visual quality is critical, such as medical imaging, surveillance, and multimedia content enhancement.

Moreover, our findings contribute to the growing body of research that explores multi-channel processing in image restoration tasks. The success of the proposed architecture suggests that further investigation into color aware network designs, including channel attention mechanisms and cross channel feature fusion strategies, could yield even greater performance gains. Future work could also explore the integration of the proposed method with real world imaging pipelines, the use of larger scale datasets, and the application of generative models or transformer-based architectures to further enhance super-resolution results.

Acknowledgement

The research and writing of this work are funded by UPNM.

References

- [1] Jalil, Muhammad Al Imraan Abdul, Puteri Zirwatul Nadila Megat Zamanhuri, Syarmela Alaauldin, and Asmalina Mohamed Saat. "Evaluation of Surface Crack Development on Marine Concrete Structure Using Matlab Image Processing." Journal of Advanced Research in Computing and Applications 21, no. 1 (2020): 1-11.
- [2] Wang, Xuan, Jinglei Yi, Jian Guo, Yongchao Song, Jun Lyu, Jindong Xu, Weiqing Yan, Jindong Zhao, Qing Cai, and Haigen Min. "A review of image super-resolution approaches based on deep learning and applications in remote sensing." Remote Sensing 14, no. 21 (2022): 5423. https://doi.org/10.3390/rs14215423
- [3] Azam, N. Z. F. N., H. Yazid, and S. A. Rahim. "Super resolution with interpolation-based method: a review." IJRAR-International Journal of Research and Analytical Reviews (IJRAR) 9, no. 2 (2022): 168-174.
- [4] Freeman, William T., Thouis R. Jones, and Egon C. Pasztor. "Example-based super-resolution." IEEE Computer graphics and Applications 22, no. 2 (2002): 56-65. https://doi.org/10.1109/38.988747
- [5] Mustafa, W. A., Yazid, H., Jaafar, M., Zainal, M., Abdul-Nasir, A. S., & Mazlan, N. (2017). A review of image quality assessment (iqa): Snr, gcf, ad, nae, psnr, me. Journal of advanced research in computing and applications, 7(1), 1-7.
- [6] Qiu, Defu, Yuhu Cheng, and Xuesong Wang. "Medical image super-resolution reconstruction algorithms based on deep learning: A survey." Computer Methods and Programs in Biomedicine 238 (2023): 107590. https://doi.org/10.1016/j.cmpb.2023.107590
- [7] Jiang, Qiuping, Zhentao Liu, Ke Gu, Feng Shao, Xinfeng Zhang, Hantao Liu, and Weisi Lin. "Single image superresolution quality assessment: a real-world dataset, subjective studies, and an objective metric." IEEE Transactions on Image Processing 31 (2022): 2279-2294.https://doi.org/10.1109/TIP.2022.3154588
- [8] Mittal, Anish, Rajiv Soundararajan, and Alan C. Bovik. "Making a "completely blind" image quality analyzer." IEEE Signal processing letters 20, no. 3 (2012): 209-212. https://doi.org/10.1109/LSP.2012.2227726
- [9] Mittal, Anish, Anush Krishna Moorthy, and Alan Conrad Bovik. "No-reference image quality assessment in the spatial domain." IEEE Transactions on image processing 21, no. 12 (2012): 4695-4708. https://doi.org/10.1109/TIP.2012.2214050
- [10] Venkatanath, Narasimhan, D. Praneeth, S. Channappayya Sumohana, and S. Medasani Swarup. "Blind image quality evaluation using perception based features." In 2015 twenty first national conference on communications (NCC), pp. 1-6. IEEE, 2015. https://doi.org/10.1109/NCC.2015.7084843
- [11] Zhai, Guangtao, and Xiongkuo Min. "Perceptual image quality assessment: a survey." Science China Information Sciences 63, no. 11 (2020): 211301. https://doi.org/10.1007/s11432-019-2757-1
- [12] Catalbas, Mehmet Cem. "Modified VDSR-based single image super-resolution using naturalness image quality evaluator." Signal, Image and Video Processing 16, no. 3 (2022): 661-668. https://doi.org/10.1007/s11760-021-02005-1
- [13] Zhang, Yunfeng, Qinglan Fan, Fangxun Bao, Yifang Liu, and Caiming Zhang. "Single-image super-resolution based on rational fractal interpolation." IEEE Transactions on Image Processing 27, no. 8 (2018):3782-3797. https://doi.org/10.1109/TIP.2018.2826139
- [14] Lee, Kwang-Chan, Guangxing Wang, and Seong-Yoon Shin. "Structure, method, and improved performance evaluation function of SRCNN and VDSR." Journal of the Korea Institute of Information and Communication Engineering 25, no. 4 (2021): 543-548.
- [15] Yamashita, Koki, and Konstantin Markov. "Medical image enhancement using super resolution methods." In *International Conference on Computational Science*, pp. 496-508. Cham: Springer International Publishing, 2020. https://doi.org/10.1007/978-3-030-50426-7_37
- [16] Pambrun, Jean-François, and Rita Noumeir. "Limitations of the SSIM quality metric in the context of diagnostic imaging." In 2015 IEEE international conference on image processing (ICIP), pp. 2960-2963. IEEE, 2015. https://doi.org/10.1109/ICIP.2015.7351345
- [17] Wang, Zhou, Alan C. Bovik, Hamid R. Sheikh, and Eero P. Simoncelli. "Image quality assessment: from error visibility to structural similarity." IEEE transactions on image processing 13, no. 4 (2004): 600-612. https://doi.org/10.1109/TIP.2003.819861
- [18] Dong, Chao, Chen Change Loy, Kaiming He, and Xiaoou Tang. "Image super-resolution using deep convolutional networks." IEEE transactions on pattern analysis and machine intelligence 38, no. 2 (2015): 295-307. https://doi.org/10.1109/TPAMI.2015.2439281
- [19] Zhang, Kai, Wangmeng Zuo, and Lei Zhang. "Learning a single convolutional super-resolution network for multiple degradations." In Proceedings of the IEEE conference on computer vision and pattern recognition, pp. 3262-3271. 2018. https://doi.org/10.1109/CVPR.2018.00344

- [20] Kim, Jiwon, Jung Kwon Lee, and Kyoung Mu Lee. "Accurate image super-resolution using very deep convolutional networks." In Proceedings of the IEEE conference on computer vision and pattern recognition, pp. 1646-1654. 2016. https://doi.org/10.1109/CVPR.2016.182
- [21] Iriyama, Taishi, Masatoshi Sato, Hisashi Aomori, and Tsuyoshi Otake. "Deep Demosaicking with Luminance and Chrominance Estimations." Journal of Signal Processing 25, no. 6 (2021): 263-268. https://doi.org/10.2299/jsp.25.263
- [22] Claßen, Tim, and Mathias Wien. "Weighted Edge Sharpening Filtering for Upscaled Content in Adaptive Resolution Coding." In 2023 IEEE International Conference on Visual Communications and Image Processing (VCIP), pp. 1-5. IEEE, 2023. https://doi.org/10.1109/VCIP59821.2023.10402728
- [23] Ganesan, P., M. Ravichandran, B. S. Sathish, LMI Leo Joseph, G. Sajiv, and R. Murugesan. "Comparative study of implementation of very deep super resolution neural network and bicubic interpolation for single image super resolution quality enhancement." In 2023 IEEE 3rd International Conference on Applied Electromagnetics, Signal Processing, & Communication (AESPC), pp. 1-7. IEEE, 2023. https://doi.org/10.1109/AESPC59761.2023.10389860